# Electronic structures of intermolecular charge-transfer states in fast electron transfers with tetrathiafulvalene donor. Thermal and photoactivation of [2 + 4] cycloaddition to *o*-chloranil acceptor†

S. V. Rosokha, S. M. Dibrov, T. Y. Rosokha and J. K. Kochi*

Tetrathiafulvalene (**TTF**) spontaneously forms a series of unusual charge-transfer complexes with various quinonoid acceptors such as *o*-chloranil (**CA**) that show pronounced near-IR absorption ($\lambda_{CT} = 1100$ nm). The successful isolation of the corresponding [1 : 1] donor–acceptor complex from solution and X-ray crystallographic analysis at low temperatures reveal the polarized charge-transfer state: [**TTF**$^{q+}$,**CA**$^{q-}$] with high degree of charge-tranfer ($q = 0.6$), which is spectrally and crystallographically distinguished from the separate redox (ion-pair) state: [**TTF**$^{+•}$ + **CA**$^{−•}$]. The unique interconversion of charge-transfer and electron-transfer states is theoretically well-accommodated by Mulliken theory using semi-empirical valence-bond and molecular-orbital methodologies. Mechanistic implications are discussed of both the thermally activated and the photochemically promoted processes *via* fast (intracomplex) electron transfer followed by collapse of the adiabatic and the non-adiabatic (vibrationally-excited) ion-pairs, respectively, to the [2 + 4] cycloadduct of tetrathiafulvalene and *o*-chloranil.

## Introduction

Transient intermolecular [1 : 1] complexes are the obligatory intermediates in the diffusive encounter of electron donors (D) with electron acceptors according to Mulliken.[1] Such [D,A] complexes are experimentally observed *via* their diagnostic charge-transfer (CT) absorption bands;[2] and they have been established as the critical (precursor) complex in intermolecular electron transfer,[3] *i.e.*

$$D + A \xrightleftharpoons{K_{CT}} [D, A] \xrightleftharpoons{K_{ET}} \left[D^+, A^-\right] \rightleftharpoons D^+ + A^- \quad (1)$$
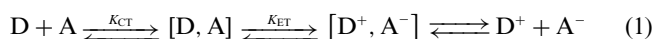
With most organic donor–acceptor dyads, the oxidation potential of the donor is considerably higher than the reduction potential of the acceptor. As such, thermal electron transfer between these redox pairs is energetically unfavorable; and observable concentrations of the ion-radical pair are attained only *via* photochemical excitation and they can lead (*via* the subsequent ion-pair dissociation) to irreversible chemical transformations,[4] *e.g.*

$$D + A \xrightleftharpoons{K_{CT}} [D, A] \xrightleftharpoons{h\nu_{CT}} \left[D^+, A^-\right] \rightarrow products \quad (2)$$
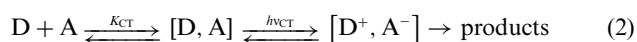
In order to evaluate experimentally the mechanistic consequences of such thermal and photochemical redox pathways, we now turn our attention to the interaction of electron donor–acceptor dyads in which a nearly isergonic electron transfer pertains. The search has led in this study to the donor–acceptor dyad consisting of tetrathiafulvalene (**TTF**) with $E_{ox}° = 0.37$ V *vs.* SCE[5] and *o*-chloranil (**CA**) with $E_{red}° = 0.15$ V *vs.* SCE, in which the redox pair: (**TTF**$^{+•}$ + **CA**$^{−•}$) has been spectrally identified earlier

to afford the covalently bonded [2 + 4] cycloadduct illustrated below (Chart 1).[6]
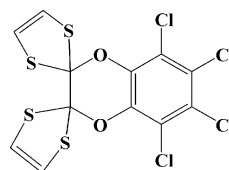


**Chart 1**

In this case, however, the authors were unable to detect the intermediate [D,A] complex; and the absence of suitable crystals ruled out the definitive X-ray structural study of the solid-state salt. As such, we will focus our attention here on the isolation, crystallization, and spectral characterization of the transient [**TTF**,**CA**] complex, and scrutinize its highly unusual electronic structure. The latter provides unique insights into the interesting mechanistic aspects of thermal and photoinduced redox transformations of organic donor–acceptor systems, particularly with regard to the role of strongly bound precursor complexes extant in thermal and photochemical processes.
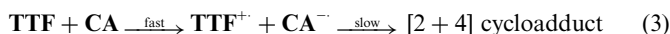
## Results

### 1.  Electronic spectroscopy of the tetrathiafulvalene–*o*-chloranil dyad

**1.1.  Spectral observation of the donor–acceptor complex and the formation of ion-radical pairs.**  The addition of *o*-chloranil to a solution of tetrathiafulvalene in acetonitrile (or *vice versa*) resulted in the immediate appearance of the twin (UV-vis) absorption bands at 450 and 580 characteristic of the **TTF**$^{+•}$ cation radical,[6]

*Department of Chemistry, University of Houston, Houston, TX, 77204, USA*
† This paper was published as part of the special issue in honour of the late Professor George S. Hammond.

*i.e.*

$$\mathbf{TTF} + \mathbf{CA} \xrightarrow{\text{fast}} \mathbf{TTF}^{+\cdot} + \mathbf{CA}^{-\cdot} \xrightarrow{\text{slow}} [2+4] \text{ cycloadduct} \qquad (3)$$

The initial electron transfer in eqn (3) was followed by the slow subsequent formation of colorless crystals of the σ-bonded [2 + 4] cycloadduct between **CA** and **TTF** shown in Chart 1.[6] However, when the same solutions were mixed at low temperature (−40 °C), careful scrutiny of the spectrum indicated the spontaneous appearance of an additional absorption in the near-IR range (∼1000 nm). If tetrathiafulvalene was added to the *o*-chloranil solution (or *vice versa*) at lower temperatures in less polar solvents such as dichloromethane, the NIR absorption was much more pronounced; and Fig. 1 illustrates the very intense (broad) band with maximum at 1100 nm which was formed immediately upon mixing the **TTF**–**CA** solutions at −90 °C. Notably, no new band characteristic of the cation radical (**TTF**⁺•) was observed in the 500–600 nm spectral range. When this solution was warmed to −50 °C, the intensity of the 1100 nm absorption decreased, but it returned to its original absorbance upon re-cooling the solution to −90 °C, which indicated that the spectral intermediate persisted and was stable at low temperatures. The application of Job's method[7] revealed that solutions with constant donor and acceptor concentrations attained a clear maximum at the equimolar ratio (left inset, Fig. 1), to establish the formation of the 1 : 1 complex according to eqn (4).
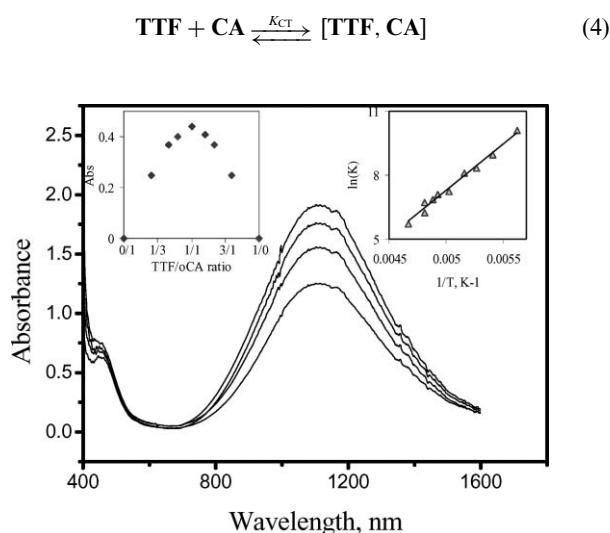
$$\mathbf{TTF} + \mathbf{CA} \xrightleftharpoons{K_{CT}} [\mathbf{TTF}, \mathbf{CA}] \qquad (4)$$



**Fig. 1** Electronic spectrum of the dichloromethane solution of **TTF** donor and **CA** acceptor (2 mM each) at 205, 194, 185 and 178 K (from bottom to top) showing strong band at 1100 nm of the [**TTF**,**CA**] complex. Inset (left): Job's plot showing maximum intensity of 1100 nm band at 1 : 1 **TTF**–**CA** concentrations ratio (at −68 °C). Inset (right): linear dependence of ln($K_{CT}$) on $1/T$.

Furthermore, the quantitative treatment of the absorption data (measured at various concentrations of **CA** and **TTF** in the temperature range from −55 to −95 °C, Fig. 1 right inset) led to the thermodynamic parameters: $\Delta H_{CT} = -8$ kcal mol⁻¹ and $\Delta S_{CT} = -28$ e.u. for the equilibrium in eqn (4). The extinction coefficient of the [**TTF**,**CA**] complex was evaluated as $\varepsilon_{CT} = 9 \times 10^3$ M⁻¹cm⁻¹ (see Experimental for details).

If the solution was warmed to higher temperatures in the range: 0 to 20 °C, the subsequent cooling resulted only in the partial

restoration of the charge-transfer (1100 nm) band to signal the occurrence of the slow irreversible [2 + 4] cycloaddition in eqn (3). Moreover, if dichloromethane solutions containing **TTF** and **CA** were kept at −20 to −30 °C for several days (in the dark, under air-free conditions), the colorless [2 + 4] adduct in Chart 1 was obtained as single crystals of the dichloromethane solvate (see Experimental for details). Notably, the photoirradiation at −78 °C of the dichloromethane solutions of [**TTF**,**CA**] (in the 700 to 1100 nm range for absorption by the complex) resulted in the formation of the same covalently bonded cycloadduct (as indicated by HPLC analysis). We thus concluded that mixtures of the **TTF** donor and the **CA** acceptor in dichloromethane led to the same redox processes as those previously described in acetonitrile.[6] However, in the less polar dichloromethane medium, the separate observation of the intermediate CT complex [**TTF**,**CA**] was readily attributable to the relatively slow rate of the subsequent electron transfer.

**1.2. Spectroscopy of other aromatic charge-transfer complexes.** Addition of hexamethylbenzene to *o*-chloranil in dichloromethane led to a new absorption band at 520 nm (Table 1) in addition to the local band of *o*-chloranil at 450 nm. The intensity of this charge-transfer band rose with the concentration of the donor or acceptor, as well as upon lowering the temperature, in accord with [1 : 1] complex formation. Additions of other organic donors to solutions of *o*-chloranil in dichloromethane afforded similar broad absorption bands. The results in Table 1 show that with weaker donors (such as benzene or toluene) the new bands were blue-shifted, and with better donors (such as octamethylbiphenylene) they were red-shifted relative to that of hexamethylbenzene. Most importantly, Fig. 2 establishes the clear Mulliken (linear) relationship of the transition energy as the function of the oxidation potential of the donor as the most distinctive feature of these charge-transfer absorptions.[1,2]
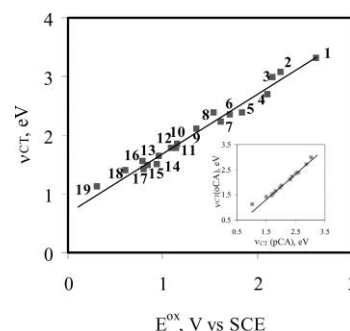


**Fig. 2** Mulliken correlation of the energy of charge-transfer transition of the complexes of *o*-chloranil acceptor with different organic donors (for donor numbering, see Table 1). Inset: correlation of energies of the *ortho*-chloranil complexes with those of *para*-chloranil.

It is noteworthy that the spectral characteristics of *o*-chloranil complexes were closely related to those of the isomeric *para*-chloranil complexes. The inset to Fig. 2 demonstrates that the charge-transfer energies with these two acceptors were linearly related to each other, with the proportionality constant of 1.0 and correlation coefficient of 0.99. Moreover, the intercept of −0.2 V indicated that the transition energies of the *o*-chloranil complexes were lower than those of the *para*-chloranil analogues; and quantitatively very close to the difference (of 0.17 V)

**Table 1** Energy of the charge-transfer transitions for intermolecular complexes of the *ortho*- and *para*-chloranil acceptors with different organic donors[a]

| N | Donor | $E^{\circ}_{ox}/V$[b] | $v_{CT}$/eV Ortho-**CA** | Para-**CA**[b] |
|---|---|---|---|---|
| 1 | Benzene | 2.6 | 3.31 | — |
| 2 | Toluene | 2.25 | 3.06 | — |
| 3 | *o*-Xylene | 2.16 | 2.98 | 3.03 |
| 4 | Mesitylene | 2.11 | 2.70 | 2.87 |
| 5 | Durene | 1.84 | 2.39 | 2.61 |
| 6 | Pentamethylbenzene | 1.71 | 2.34 | 2.53 |
| 7 | Hexamethylbenzene | 1.62 | 2.22 | 2.39[e] |
| 8 | Naphthalene | 1.54 | 2.39 | 2.58[e] |
| 9 | Anthracene | 1.09 | 1.77 | 1.97 |
| 10 | 2,6-Dimethylnaphthalene | 1.36 | 2.10 | 2.32 |
| 11 | Pyrene | 1.16 | 1.85 | 2.03 |
| 12 | 2,5-Dimethyl-*p*-dimethoxybenzene | 1.15 | 1.78 | — |
| 13 | 9-Methylanthracene | 0.96 | 1.64 | 1.83 |
| 14 | 9,10-Dimethylanthracene | 0.94 | 1.50 | 1.69 |
| 15 | Perylene | 0.85 | 1.48 | 1.69 |
| 16 | Octamethylbiphenylene | 0.80 | 1.41 | 1.51[d] |
| 17 | 10-Methylphenothiazine | 0.79[c] | 1.55 | — |
| 18 | Phenothiazine | 0.61[c] | 1.39 | — |
| 19 | Tetrathiafulvalene | 0.37 | 1.13 | 1.03[d] |

[a] In dichloromethane, at 22 °C, unless noted otherwise. (Note the spectral data in Table 1 are close to those measured earlier for some of the corresponding complexes with aromatic donors in CCl₄[8]). [b] From ref. 9 unless noted otherwise. [c] From ref. 10. [d] This work.

in their reduction potentials. Most importantly, the complexes of the tetrathiafulvalene donor with each of these (*para*- or *ortho*-chloranil) acceptors fell on the corresponding Mulliken correlation (with deviations comparable to those observed with other donors) to provide unambiguous indication of their charge-transfer character.

## 2. X-Ray crystallography of the [TTF,CA] complex and related systems

**2.1. General structural characterization of the [TTF,CA] complex in comparison with related charge-transfer complexes.** Slow diffusion of the hexane solution of tetrathiafulvalene into the dichloromethane solution of *o*-chloranil at −65 °C led to black crystals, and X-ray crystallographic analysis (see Experimental) established the 1 : 1 stoichiometry with alternating stacks of *o*-chloranil positioned over one side of the tetrathiafulvalene stacks (Fig. 3). The close interplanar separation of about 3.0 Å with intermolecular C···S atomic contacts of only 2.98 Å (as compared to the sum of their van der Waals radii of 3.55 Å) identified the existence of strong donor–acceptor interactions within this complex.

To further elucidate the [TTF,CA] complex, we first carried out a crystallographic comparison of the charge-transfer associates of the **CA** acceptor with other donors, as well as the **TTF** donor with other acceptors. Although the Cambridge Structural Database[11] contains numerous examples of tetrathiafulvalene complexes, the structures of the *o*-chloranil associates with other organic π-donors are singularly absent. We thus prepared single crystals of *o*-chloranil complexes with durene and pyrene, as representative aromatic donors. X-Ray analysis revealed that both complexes showed alternating donor–acceptor stacks with 1 : 1 stoichiometry in the case of **CA**–durene crystals, and 2 : 3 acceptor–donor ratio in the **CA**–pyrene system (in which additional donors are arranged between columns). While such stacks were similar to that formed in the *o*-chloranil complex with **TTF**, the associates with pyrene and durene were both characterized by significantly larger interplanar separations of $r_{DA} \approx 3.4$ Å (characteristic of most charge-transfer complexes[12]) compared to $r_{DA} \approx 3.0$ Å in the [TTF,CA] complex. In a similar way, the latter was significantly closer than the separation of 3.5 Å in complexes of **TTF** with weaker acceptors, including *para*-chloranil.[13–15] As such, these general structural comparisons indicated that the very close donor–acceptor separation that characterizes the [TTF,CA] complex was
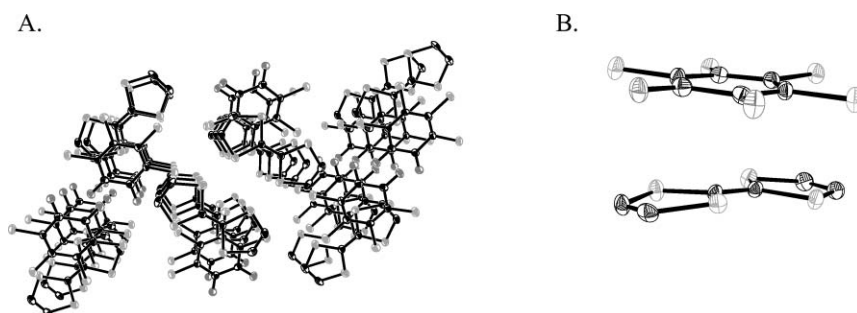


**Fig. 3** (A) Crystal lattice of the [**TTF,CA**] complex showing alternating donor–acceptor stacks. (B) Side perspective view of the [1 : 1] complex.

indicative of very strong interactions between the donor–acceptor moieties.

To reveal the structural effect of such enhanced donor–acceptor interaction on each of the constituents, we also compared the molecular geometries of the **TTF** and **CA** moieties with those present in other charge-transfer complexes, as well as in the corresponding neutral parents and their ion-radicals salts.

### 2.2. Structural characterization of TTF and CA moieties.

The structural characteristics of the *o*-chloranil and tetrathiafulvalene moieties are presented in Table 2. In order to make the comparison quantitative relative to the neutral and ionic analogues, we first re-measured the X-ray structure of *o*-chloranil (Table 2) to provide the structural basis for the neutral donor and acceptor counterparts (together with the literature data).
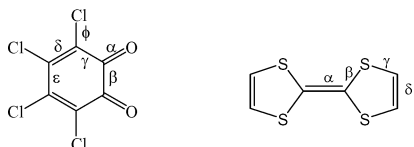
The synthesis and X-ray analysis of the tetrathiafulvalene salt with dodecamethylcarborane anion, **TTF$^{+\bullet}$CB$^-$**, provided the basic structural information concerning the cation-radical moiety. Thus the tetrathiafulvalene cation within this salt was very close to being a "free" species since: (i) **TTF$^{+\bullet}$** bears a full unit charge in this outer-sphere salt, in contrast to those cations included in the literature data dealing with mixed-valence salts;[11] (ii) no dimerization occurs in this salt (as opposed to such structures extant in other [1 : 1] tetrathiafulvalene salts which can also lead to cation distortion); (iii) the interchangeable **TTF$^{+\bullet}$/CB$^-$** pairs and charge delocalization within the bulky counteranion[16] minimized any electrostatic interactions and external geometry distortions of the cation-radical species. Notably, the recrystallization of the **TTF$^{+\bullet}$CB$^-$** salt from diethyl ether afforded the corresponding ethereal solvate, but the geometry of the **TTF$^{+\bullet}$** moiety (Table 2) was the same as that in the pure **TTF$^{+\bullet}$CB$^-$** salt. In fact, the centrosymmetric cation radical was characterized by an essentially planar geometry showing an elongated central double bond and significantly shortened C–S bonds in Table 2, which were close to the average values for the corresponding bondlengths taken over an extended set of different salts with different counterions.[19] [However the latter showed rather wide variations of up to 0.02 Å[19] due to crystal-packing interferences.]

Since the crystallographic data for the *o*-chloranil anion radical were unavailable in the literature (and our efforts to prepare single crystals suitable for X-ray crystallography were unsuccessful), we evaluated its structure (Table 2) *via* DFT calculations with the aid of Gaussian 98.[20] (Note that the analogous computation of neutral *o*-chloranil resulted in structural parameters which were within one standard deviation of those observed in different X-ray structures).

### 2.3. Evaluation of the degree of charge-transfer in the [TTF,CA] complex.

Consideration of the molecular geometries of both tetrathiafulvalene and *o*-chloranil in the [**TTF**,**CA**] complex revealed that they differed significantly from those extant in the neutral donor or acceptor and in related CT complexes with significantly weaker donor and acceptors. For example, the C=O and C=C bonds in the chloranil moiety in the [**TTF**,**CA**] complex (Table 2) were longer than the corresponding bond parameters in neutral **CA** and in either the [durene,**CA**] or [pyrene,**CA**] complexes; and the corresponding C–C single bonds were also shorter. Indeed, the geometry of the former was *intermediate* between those in the neutral *o*-chloranil and its anion-radical, to suggest the presence of significant charge transfer from the donor to the acceptor. This conclusion was supported by the lengthened central C=C bond and the shortened (adjusted) C–S bond in the complexed tetrathiafulvalene relative to that in the parent (neutral) **TTF**—to also indicate partial oxidation of the former.

**Table 2** Average bondlengths$^a$ (Å) within *o*-chloranil and tetrathiafulvalene moieties in the [**TTF**,**CA**] complex in comparison with those in related neutral molecules, ion-radicals and CT complexes

| Structure | α | β | γ | δ | ε | φ$^a$ |
|---|---|---|---|---|---|---|
| *o*-Chloranil moieties | | | | | | |
| **CA**$^b$ | 1.209(6) | 1.549(6) | 1.474(8) | 1.350(6) | 1.476(6) | 1.705(6) |
| **CA$^{-\bullet}$**$^c$ | 1.234 | 1.517 | 1.453 | 1.381 | 1.425 | 1.758 |
| **CA**–**TTF** | 1.226(6) | 1.514(5) | 1.447(4) | 1.357(5) | 1.446(5) | 1.720(6) |
| **CA**–durene | 1.208(2) | 1.544(2) | 1.470(2) | 1.348(3) | 1.473(2) | 1.703(3) |
| **CA**–pyrene$^d$ | 1.206(6) | 1.555(5) | 1.472(7) | 1.349(7) | 1.475(4) | 1.706(6) |
| Tetrathiafulvalene moieties | | | | | | |
| **TTF**$^e$ | 1.349(3) | 1.759(2) | 1.742(6) | 1.329(9) | — | — |
| **TTF$^{+\bullet}$**$^f$ | 1.396(4) | 1.716(5) | 1.726(4) | 1.334(6) | — | — |
| **CA**–**TTF** | 1.373(4) | 1.732(5) | 1.725(8) | 1.337(5) | — | — |
| *p*-**CA**–**TTF**$^g$ | 1.353 | 1.750 | 1.737 | 1.313 | — | — |
| BQ–**TTF**$^h$ | 1.341 | 1.757 | 1.731 | 1.315 | — | — |
| *m*-DNB–**TTF**$^i$ | 1.345 | 1.761 | 1.734 | 1.324 | — | — |

$^a$ In parentheses—standard deviations calculated based on both the esd of individual bondlengths (see CIF files) and variations of particular (but crystallographically non-equivalent) bonds in one or several (as indicated) structures. $^b$ Averaged over 8 crystallographically independent molecules in two different X-ray structures measured in this work. $^c$ From DFT calculations. $^d$ Averaged over 4 crystallographically independent molecules. $^e$ Averaged over 5 molecules from structures in ref. 18. $^f$ Averaged over 2 molecules from 2 structures (as salt with CB$^-$ counterion) measured in this work. $^g$ Neutral phase, from ref. 15. $^h$ Complex with benzoquinone, from ref. 14. $^i$ Complex with *m*-dinitrobenzene, from ref. 13.

Bondlength measurements in conjunction with the classic Pauling bondlength/bondorder relationship,[21] have often been used for the evaluation of degree of charge transfer,[22] particularly in those complexes involving tetrathiafulvalene.[17,19] Accordingly, we first estimated the charge ($q$) on the basis of eqn (5):

$$q = 1/n \sum q^i = 1/n \sum (l_{CT}^i - l_0^i)/(l_1^i - l_0^i) \qquad (5)$$

where $l_{CT}^i$, $l_0^i$ and $l_1^i$ were the $i$th bondlengths in the donor moiety within the CT complex, neutral molecule and cation radical, respectively, from Table 2 (so that the value $q^i = (l_{CT}^i - l_0^i)/(l_1^i - l_0^i)$ provided the estimate based on a particular bond), and $n$ was the number of equivalent bonds. Thus, the overall charge on the **TTF** moiety in the charge-transfer complex was evaluated as $q = 0.77 \pm 0.27$ based on the $\alpha$, $\beta$ and $\gamma$ bonds (which show significant changes upon 1-electron oxidation). Notably, the earlier suggested[17] estimate based solely on C–S bond "$\beta$" produced the value of $q = 0.62 \pm 0.14$ (Table 3). For comparison, the degree of charge transfer in tetrathiafulvalene complexes with weaker acceptors such as *m*-dinitrobenzene and *p*-benzoquinone were evaluated to be essentially nil (Table 3).

Similar analysis of the *o*-chloranil moiety in the [**TTF**,**CA**] complex led *via* eqn (5) to the charge of $q = -0.6$ (in comparison to neutral and anionic *o*-chloranil), whereas in CT complexes with weaker donors, the value of $q$ was evaluated as essentially 0. Notably, these calculations (with relatively high estimated standard deviations) were consistent with the most accurate evaluation of the charge residing on the tetrathiafulvalene of $0.62 \pm 0.14$ using the C–S bondlength "$\beta$" according to ref. 17. In summary, the structural analyses have led to the conclusion that $q = 0.6 \pm 0.1$ is our most reliable estimate of the degree of charge transfer within the [**TTF**,**CA**] complex.

It noteworthy that the extensive charge-transfer within the [**TTF**,**CA**] complex was in strong contrast to the essentially neutral *o*-chloranil or tetrathiafulvalene moieties present in those associates with weaker donors or acceptors. Interestingly, the value of $q = 0.6$ was intermediate between the value of $q = 0.4$ (estimated at room temperature) and $q = 0.8$ (estimated at 40 K) for the neutral and ionic phases, respectively, of the isomeric complex of tetrathiafulvalene with the *para*-chloranil evaluated earlier.[19] We thus believe that the considerable degree of charge-transfer was related to the strong donor–acceptor interactions extant within the [**TTF**,**CA**] complex, as also evident from the close intermolecular donor–acceptor contacts present in the unit cell (Fig. 3, left).

**Table 3** Estimate of the charge residing on the tetrathiafulvalene and *o*-chloranil moieties[a] in their complex in comparison with those in complexes with weaker acceptor or donor counterparts

| Complex | $q$ (**TTF**) | Complex | $q$ (**CA**) |
|---|---|---|---|
| [**TTF**,**CA**] | $0.76 \pm 0.25(0.62 \pm 0.14)^b$ | [**TTF**,**CA**] | $-0.60 \pm 0.40$ |
| [**TTF**,*m*-DNB] | $0.15 \pm 0.29(0.02 \pm 0.13)$ | [Durene,**CA**] | $-0.02 \pm 0.10$ |
| [**TTF**,*p*-BQ] | $0.23 \pm 0.37(-0.06 \pm 0.13)$ | [Pyrene,**CA**] | $0.02 \pm 0.09$ |

[a] According to eqn (5), using **CA** and **TTF** bonds showing bondlength differences which exceed significantly the standard deviations. [b] In parentheses—estimation based on C–S bondlength variation.

## Discussion

Spectral identifications, coupled with the isolation and X-ray crystallographic analysis of the [1 : 1] charge-transfer complex of tetrathiafulvalene (**TTF**) and *ortho*-chloranil (**CA**), as well as those in the corresponding ion-radical pair [**TTF**[+•] + **CA**[−•]] provide unambiguous confirmation of the coupled set of charge-transfer ($K_{CT}$) and electron-transfer ($K_{ET}$) equilibria according to eqn (1) with D = **TTF** and A = **CA**. Furthermore, the actinic activation of the [2 + 4] cycloaddition by direct irradiation ($h\nu_{CT}$) of the intervalence absorption band according to eqn (2) interconnects the thermal (adiabatic) with the photochemical (non-adiabatic) electron-transfer processes *via* the critical [1 : 1] charge-transfer complex.

Although a wide variety of analogous charge-transfer complexes of organic π-donors and π-acceptors have been characterized,[1,2] the [1 : 1] complex of tetrathiafulvalene and *o*-chloranil is rather unique in that it is comprised of an unusually strong pair of donor–acceptor components in which the free-energy change for electron transfer as given by: $E_{ox}^{TTF} - E_{red}^{CA} = 0.22$ V corresponds to a slightly endergonic process with driving force of only $\Delta G_{ET} = 5.2$ kcal mol$^{-1}$. As such, the electronic structure of this relatively strong complex with $\Delta H_{CT} = -8$ kcal mol$^{-1}$ and $\Delta S_{CT} = -28$ e.u. has important mechanistic implications that can be analyzed as follows.

### 3. Electronic coupling element ($H_{ab}$) in the tetrathiafulvalene complex with *o*-chloranil

All the separate thermodynamics, spectral and structural data that are now available for the [1 : 1] complex allow two independent semi-empirical methodologies to be employed in the theoretical evaluation of the charge-transfer complex *via* the electronic coupling element.

**3.1. Valence-bond and molecular-orbital formulations of charge-transfer complexes.** In the general context of Mulliken valence-bond theory, the ground-state and excited-state wave functions consist of linear combinations of the principal van der Waals (D/A) state $\psi_a$ and the dative (D$^+$/A$^-$) state $\psi_b$:[1,3,23,24]

$$\psi_{GS} = a\psi_a + b\psi_b \qquad (6a)$$

$$\psi_{ES} = a'\psi_a + b'\psi_b \qquad (6b)$$

with the normalization restriction: $a^2 + b^2 = 1$. Within the alternative molecular-orbital approach, $\Psi_{GS}$ and $\Psi_{ES}$ are expressed in the same way *via* the HOMO of the donor and the LUMO of the acceptor. The solution of the corresponding secular determinant leads to the ground-state and excited-state energies as:[23]

$$E_{GS} = (H_{aa} + H_{bb})/2 - ((H_{bb} - H_{aa})^2 + 4H_{ab}^2)^{1/2}/2 \qquad (7a)$$

$$E_{ES} = (H_{aa} + H_{bb})/2 + ((H_{bb} - H_{aa})^2 + 4H_{ab}^2)^{1/2}/2 \qquad (7b)$$

where $H_{aa} = \int \psi_a H \psi_a$ and $H_{bb} = \int \psi_b H \psi_b$ represent the energies of the initial and final diabatic states (or HOMO/LUMO energies in molecular-orbital terms). $H_{ab} = \int \psi_a H \psi_b$ is the electronic coupling element (exchange integral), and the orbital overlap is neglected ($\int \psi_a \psi_b = 0$). Thus, the energy of the optical transition is:

$$\nu_{CT} = E_{ES} - E_{GS} = ((H_{bb} - H_{aa})^2 + 4H_{ab}^2)^{1/2} \qquad (8)$$

and the solution of eqn (6a) and (6b) with these eigenvalues leads to the coefficients that determine the donor–acceptor electron distribution that are linked as: $a' = b$, and $b' = -a$; and these coefficients are related to the coupling element as:[23]

$$|ab| = |H_{ab}|/(E_{ES} - E_{GS}). \qquad (9)$$

The molecular-orbital diagram of the donor–acceptor dyad is presented in Chart 2.



**Chart 2**
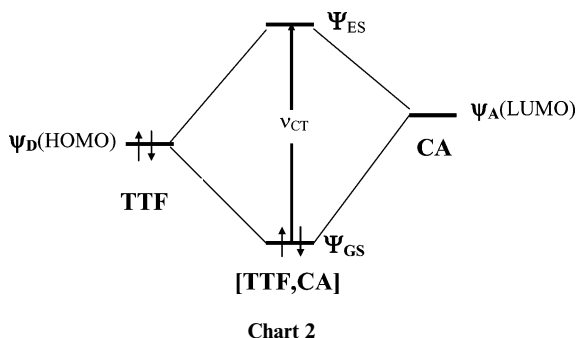
### 3.2. Mulliken–Hush evaluation of the electronic coupling element in the [TTF,CA] complex.

The theoretical formalism identifies the electronic coupling element $H_{ab}$ as the crucial parameter determining the electronic characteristics of the donor–acceptor dyad. Experimentally, it can be evaluated from the intensity integral of the intervalence absorption *via* the Mulliken–Hush expression:[1,25]

$$H_{ab} = 0.0206(v_{CT}\Delta v_{1/2}\varepsilon_{CT})^{1/2}/r_{DA} \qquad (10)$$

where $v_{CT}$ and $\Delta v_{1/2}$ are the spectral maximum and full-width at half maximum $(cm^{-1})$, respectively, of the charge-transfer absorption band, $\varepsilon_{CT}$ is the extinction coefficient $(M^{-1}\ cm^{-1})$ of the precursor complex, and $r_{DA}$ is the separation (Å) between the redox centers. Although this expression was derived originally for weakly-interacting mixed-valence complexes, Creutz, Newton and Sutin showed its applicability, within the intermolecular two-state model, to strongly interacting systems.[23] Thus, the spectral and structural characteristics of the [**TTF**,**CA**] complex provide all the parameters for eqn (6) using $v_{CT} = 9.1 \times 10^3\ cm^{-1}$, and $\Delta v_{1/2} = 3.2 \times 10^3\ cm^{-1}$ $\varepsilon_{CT} = 9 \times 10^3\ M^{-1}\ cm^{-1}$ and $r_{DA} = 2.9$ Å; and the Mulliken–Hush formalism thus leads to $H_{ab} = 3.5 \times 10^3\ cm^{-1}$.

### 3.3. Structural validation of the electronic coupling in [TTF,CA] complex.

The electron population on donor–acceptor sites (as reflected by the coefficients $a$ and $b$) is related directly to the coupling element and the difference between the ground and excited state energies according to eqn (9). Taking into account that the $(E_{ES} - E_{GS})$ difference is readily measured experimentally as the absorption maximum $(v_{CT})$ of the charge-transfer band, the experimental determination of charge transfer provides the independent evaluation of the coupling element $H_{ab}$. Thus, the charge transferred from the **TTF** (donor) to **CA** (acceptor), experimentally evaluated by the degree of charge transfer $(q)$ in eqn (5), is identified in Mulliken theory by the coefficients in eqn (6) so that: $q = 2b^2$ by definition (see Experimental); and this leads to $H_{ab}$ in eqn (9) as:

$$H_{ab} = v_{CT}[(1 - q/2)q/2]^{0.5} \qquad (11)$$

Accordingly, the experimental values of $v_{CT}$ and $q$ (*vide supra*) together yield: $H_{ab} = 4.1 \times 10^3\ cm^{-1}$, in good agreement with the Mulliken–Hush evaluation above.

It must be stressed that the evaluations of the electronic coupling element *via* eqn (10) and (11) are based on the independent sets of spectral and structural data. Thus, the Mulliken–Hush eqn (10) is based on the integral intensity (transition moment) of the intervalence band, and the donor–acceptor separation within complex. On the other hand, the Mulliken eqn (11) is based on the charge transfer in the ground state determined experimentally from the molecular structure of the donor–acceptor moieties and the energy of charge-transfer transition. The fact that these independent evaluations lead to essentially the same value of: $H_{ab} = (3.8 \pm 0.3) \times 10^3\ cm^{-1}$ supports the reliability and consistency of our evaluation and leads to the next step—the evaluation of the potential—energy surface along the electron-transfer coordinate stemming from the single-point analysis of the ground-state minimum as presented in this section. Hush[25] and Brunschwig and Sutin[26] showed that such a surface can be constructed by the combination of the Mulliken formalism[1] with the Marcus representation of the initial and final diabatic states *via* the reorganization energy $(\lambda)$ and the free-energy change $\Delta G_{ET}$ for electron transfer[27] as follows.

## 4. Potential energy surface for thermal and optical electron transfer

### 4.1. Evaluation of the reorganization energy $(\lambda)$

The overall reorganization energy $(\lambda)$ for electron transfer consists of intramolecular and solvent components. The intramolecular component $(\lambda_i)$ of the reorganization energy for electron transfer within the donor–acceptor complex can be calculated as the difference between the energy of the initial (diabatic) state in which the electron is located on donor and the reactants are in their relaxed nuclear geometries *versus* the energy of the final (diabatic) state in the same nuclear geometry, but with electron transferred from the donor to the acceptor.[28] We first optimize the geometry for the neutral and cationic tetrathiafulvalenes and determine their energies, $E_n(r_n)$ and $E_c(r_c)$ *via* DFT computations (6–311G* basis and B3LYP functional) with Gaussian 98.[20] Then, the single-point calculation of **TTF$^{+\bullet}$** in the geometry of neutral **TTF** leads to $E_c(r_n)$. Analogous computations of the neutral **TTF** in the geometry of the cation produces $E_n(r_c)$; and the energy difference leads to: $\lambda_i^{TTF} = 2.3 \times 10^3\ cm^{-1}$. The same procedure with the neutral and anionic **CA** results in: $\lambda_i^{CA} = 3.9 \times 10^3\ cm^{-1}$. As such, the inner-sphere (vibrational) reorganization is calculated as: $\lambda_i = (\lambda_i^{CA} + \lambda_i^{TTF})/2 = 3.1 \times 10^3\ cm^{-1}$.

To calculate the solvent component $(\lambda_o)$, the charge-transfer complex is considered as a cavity with an internal dielectric constant of $\varepsilon_{in} = 2$ immersed in a solvent with static and optical dielectric constants $\varepsilon_s$ and $\varepsilon_o$.[28] In the Kirkwood solvation model, the reorganization energy is:[29]

$$\lambda_o = 1/2a_0\{(1/\varepsilon_{in} - 1/\varepsilon_s)\sum_n g_n/(1 + [n/(n+1)]\varepsilon_{in}/\varepsilon_s)$$

$$- (1/\varepsilon_{in} - 1/\varepsilon_o)\sum_n g_n/(1 + [n/(n+1)]\varepsilon_{in}/\varepsilon_o)\} \qquad (12)$$

where $g_n = \sum_{k,j}^{N} \Delta e_k \Delta e_j (r_k/a_0)^n (r_j/a_0)^n P_n(\cos\theta_{jk})$, with $n = 1$ to 6. The term $\Delta e_j$ denotes the ET-induced variation of charge on the

$j$th atom, $N$ is number of atoms, $r_j$ locates the $j$th atom in space, $\theta_{jk}$ is the angle between $r_j$ and $r_k$, and $P_n$ are ordinary Legendre functions. The atomic coordinates in the precursor complex are taken from the X-ray structures of [**TTF**,**CA**] and the value of $a_0 = 5.2$ Å is calculated from the molecular volume of this dyad (from the single-point Gaussian 98 computation plus 0.5 Å).[28] The atomic charges on the neutral molecules and the corresponding ion-radical pair constituting the complex in the hypothetical diabatic states are taken from the Gaussian 98 computation of the isolated species (ESP charges, CHELPG option[20]). This procedure results in the solvent reorganization of $\lambda_o = 1.7 \times 10^3$ cm$^{-1}$ and, together with the inner-sphere component, leads to total reorganization energy of: $\lambda = 4.8 \times 10^3$ cm$^{-1}$ for the electron transfer within the [**TTF**,**CA**] complex in dichloromethane solution.

### 4.2. Construction and spectral validation of the two-state energy diagram

As described in previous sections, the electron transfer within [**TTF**,**CA**] complex is characterized by (i) the coupling element: $H_{ab} = 0.47$ eV ($3.8 \times 10^3$ cm$^{-1}$) (*vide supra*); (ii) the Marcus reorganization energy: $\lambda = 0.60$ eV ($4.8 \times 10^3$ cm$^{-1}$) theoretically computed from the inner-sphere and solvent reorganization components, and (iii) the free-energy change of: $\Delta G_{ET} = F\Delta E = 5.2$ kcal mol$^{-1} = 0.22$ eV calculated from the difference of the reversible redox potentials of the **TTF**–**TTF**$^{+\bullet}$ and **CA**$^{-\bullet}$–**CA** couples (since $\Delta G_{ET}$ corresponds to the energy difference between diabatic states, *i.e.* the non-interacting neutral molecules and the ion-radical pairs). The diabatic-state energies: $H_{aa}$ and $H_{bb}$ are calculated from the values of $\Delta G_{ET}$ and $\lambda$ following Brunschwig and Sutin[26] as: $H_{aa} = \lambda X^2$ and $H_{bb} = \Delta G_{ET} + \lambda(X-1)^2$, where $X$ represents the reaction coordinate shown as gray curves in Fig. 4. The electronic coupling energy of such diabatic states with the constant value of the coupling element $H_{ab}$ at each point of the reaction coordinate [in other words, the solution of the eqn (7) with $H_{aa} = \lambda X^2$, $H_{bb} = \Delta G_{ET} + \lambda(X-1)^2$ and $H_{ab}$ at various $X$] results in the energies of the adiabatic ground and excited states presented in Fig. 4 as the lower and upper black curves, respectively.
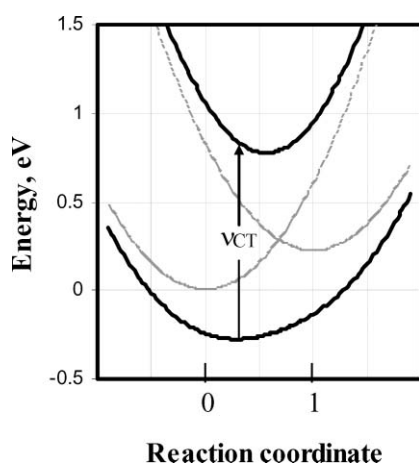


**Fig. 4** Two-state energy diagram for the electron-transfer in the [**CA**,**TTF**] dyad with diabatic states (in gray) and with the single-minimum ground and excited states (in black).

The potential-energy diagram in Fig. 4 demonstrates that the strong donor–acceptor electronic coupling (as reflected by the large value of $H_{ab}$) results in a broad single-minimum ground state at $X = 0.25$; and the ground- and excited-state energy difference at this point is $8.7 \times 10^3$ cm$^{-1}$. Since the latter represents the energy of the optical (electronic) transition within the donor–acceptor associate, it is especially important to note that it is closely correlated (within 5%) with the experimentally measured maximum of the charge-transfer band ($9.1 \times 10^3$ cm$^{-1}$)—to provide the critical validation of the two-state model as applied to the [**TTF**,**CA**] complex. Such a consistency of the spectral and structural descriptions of the [**TTF**,**CA**] complex *via* the Marcus–Hush model with experiment allows us to draw some interesting mechanistic conclusions about thermal and optical electron-transfer processes in such a system as follows.

## 5. Mechanistic implications of thermal and photochemical electron transfer *via* strongly bound charge-transfer complexes

### 5.1. Adiabatic electron transfer within the ground-state [TTF,CA] complex

According to Mulliken,[1] the diffusive association of tetrathiafulvalene with *o*-chloranil occurs spontaneously with no or little activation energy, as observed by the immediate appearance of the diagnostic charge-transfer absorption band at $\lambda_{CT} = 1100$ nm in Fig. 1 upon mixing the donor–acceptor components. This barrierless (bimolecular) process leads directly to the single-minimum ground-state shown in Fig. 4 involving extensive electron-pair redistribution—the ground state wave function $\Psi_{GS}$ being described as a linear combination of the donor HOMO and acceptor LUMO with coefficients $a$ and $b$, respectively. As such, the excess electron-density distribution on the chloranil LUMO reflects the degree of charge transfer and it is evaluated as the measured quantity: $q = 2b^2$. As the result of the extensive electron-pair redistribution, more than half an electron is transferred from the tetrathiafulvalene HOMO to the *o*-chloranil LUMO in spite the fact that the driving force for the electron transfer from **TTF** to **CA** is endergonic. Furthermore, the strong donor–acceptor interaction eliminates the activation barrier for the thermal electron transfer step within the [**TTF**,**CA**] complex according to the energy diagram in Fig. 4. Thus, in terms of the traditional Robin–Day classification,[30] the **TTF**–**CA** dyad corresponds to a Class III delocalized system; and the separate precursor and successor complexes in eqn (1) must be replaced by a single intermediate with a high degree of charge transfer *i.e.*

$$\text{D} + \text{A} \xrightarrow{K_{CT}} [\text{D}^{q+}, \text{A}^{q-}] \rightleftarrows \text{D}^+/\text{A}^- \qquad (13)$$
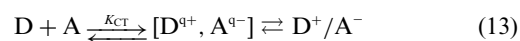
where $q \approx 0.6$. [In the similar way, the high degree of ground-state charge transfer and the elimination of the barrier for electron transfer were established earlier for the strongly-coupled charge-transfer complexes of the nitrosonium cation with various aromatic donors.[31]]

The overall electron-transfer process is best described as the initial formation of a tight π-bonded complex followed by its homolytic dissociation into the adiabatic or thermally equilibrated ion-radical pair (in contrast to a heterolytic dissociation reverting

to the starting donor–acceptor dyad). The follow-up reaction of the ($TTF^{+\bullet}$ + $CA^{-\bullet}$) radical pair leads to the thermodynamically most stable products (Chart 1). The free-energy diagram for such electron-transfer mediated process is qualitatively depicted in Chart 3 based on the quantitative potential-energy surface for the diffusion-controlled formation of charge-transfer complex presented in Fig. 4. According to Chart 3, the rate of the [2 + 4] cycloaddition process is limited by the activation energy $\Delta G_{IP}^{\neq}$ for the ion-pair collapse to the cycloadduct plus the driving force $\Delta G_{ET}$ for the redox transformation of the tetrathiafulvalene–*o*-chloranil dyad, and most unexpectedly, it is *unaffected* by the stability of the precursor complex despite its high degree of charge transfer. [The latter is of course critical to its belonging to Robin–Day Class III and not to Class II.]
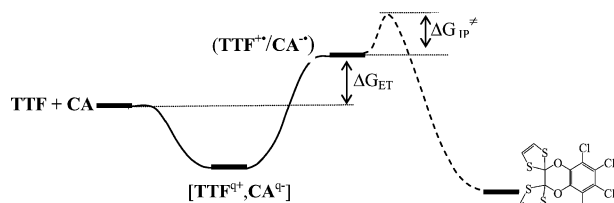


**Chart 3**

Organic donor–acceptor electron-transfer processes *via* the charge-transfer complex in Chart 3 are quite similar to inorganic inner-sphere electron-transfer reactions in which the redox-process also involves bond-formation/dissociation and are mediated by the bonding of the pair of redox centers *via* the (covalent) coordination of a bridging ligand.[32] In the same way, it is related to redox-reactions between organic radicals proceeding *via* addition/elimination (inner-sphere) pathways described by Steenken.[33] However, owing to the even number of electrons on the HOMO/LUMO orbitals, the association in charge-transfer complexes is akin to the formation of a discrete dative bond. [Due to the delocalized nature of such a π-bonding, the equilibrium donor–acceptor separation is only moderately (0.3–0.5 Å) shorter than the sum of corresponding van der Waals radii.[34]] Most notably, the overall single-electron transfer corresponds to an electron-pair "redistribution", and, as such, the novel mechanism presented in Chart 3 blurs the traditionally sharp distinction between polar and single-electron transfer mechanisms.[35]

### 5.2.  Photo-population of the excited charge-transfer state and ion-pair collapse to the cycloadduct

According to Mulliken theory,[1] photoexcitation of donor–acceptor complexes by direct irradiation of the charge-transfer absorption band corresponds to electron transfer to the excited ion-pair state; and time-resolved (ps) spectroscopy has confirmed the transient formation of the donor cation-radical ($D^{+\bullet}$) together with the acceptor anion-radical ($A^{-\bullet}$).[4,36] Such a non-adiabatic transformation within weak complexes (in which the coefficients: $a \gg b$ in eqn (6) is related to the low degree of charge transfer in the ground state with $q = 2b^2 \approx 0$ and to the highly polarized excited state with $q = 1.0$.[1] However, in the case of the strongly-coupled **TTF–CA** dyad of interest here, the high degree of charge-transfer with $q = 0.6$ indicates that the tetrathiafulvalene moiety is already more than half way towards its cation-radical, and the acceptor

moiety is equally transformed to the chloranil anion radical. The existence of such a strong ground-state polarization thus raises the question as to the mechanistic significance of the electronic (optical) transition corresponding to the charge-transfer band. In order to address this potential ambiguity, let us return to the Mulliken formulation in eqn (6), and we evaluate the acceptor coefficients as $b = (0.5q)^{0.5} = 0.55$ and the donor coefficient as $a = (1 - b^2)^{0.5} = 0.84$, based on the structural data and the normalization restriction. Thus Mulliken theory predicts that the ground-state wavefunction for the **TTF–CA** dyad is characterized by the prevailing contribution of the HOMO (donor) and the excited state is centered on the LUMO (acceptor). However, owing to the *electron-pair* involvement, the electron population in the ground state is centered on the LUMO(acceptor), as indicated by $q = 0.6$. The promotion of one electron to the excited state during optical excitation leads to the increase of electron population on the acceptor, so that the overall extent of charge transfer in the excited state is: $q' = 1$. Notably, the Mulliken (two-state) representation predicts that charge-transfer excitation *always* produces the excited state with an integral number of (2) electrons equally distributed between the donor–acceptor dyads *irrespective of the ground-state charge distribution*. In other words, the optical excitation results in one electron on $\Psi_{GS}$ (with the contribution of the acceptor LUMO of $b'^2$), together with one electron on the excited-state wavefunction with the contribution of the acceptor LUMO, such that $a'^2 = 1 - b'^2$. Since the optical transition breaks the electron-pair in the ground state to produce one electron in the bonding orbital, and the other in the antibonding orbital, the resulting excited-state dyad (consisting of the oxidized donor and the reduced acceptor) is essentially non-bonded, and readily dissociates into the ion-pair shown in Chart 4.
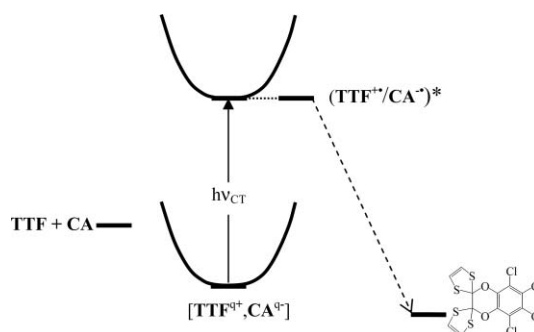


**Chart 4**

According to Chart 4, the photoactivation of the **TTF–CA** dyad initially affords the non-adiabatic (vibrationally excited) ion-pair at roughly 14 kcal mol$^{-1}$ higher than the adiabatic ion-pair in Chart 3. As such, ion-pair relaxation is expected to be fast and likely lead directly to the [2 + 4] cycloadduct—as qualitatively depicted in Chart 4 where $h\nu_{CT} = 27$ kcal mol$^{-1}$ (and with $\Delta G_{ET} = 5.2$ kcal mol$^{-1}$ and $\Delta G_{CT} = 8.0$ kcal mol$^{-1}$). Furthermore, a preliminary assessment of the quantum yield for this overall photochemical process suggests that such an ion-pair annihilation occurs with little or no activation energy; but more quantitative (actinometric) measurements will be required to evaluate its branching ratio relative to back electron transfer.

# Experimental

## Materials

Tetrathiafulvalene, *o*- and *p*-chloranil from commercial sources were purified by sublimation *in vacuo*, and the other donors in Table 1 were used without additional purification. The (**TTF⁺•CB⁻**) salt was produced by oxidation of **TTF** with a stoichiometric (1 : 1) amount of dodecamethylcarboranyl radical CB• (prepared by oxidation of Cs⁺CB⁻ with PbO₂[16]) in dichloromethane, and precipitated with hexane. Solvents were prepared and handled as described earlier.[10]

## Spectral (UV-vis-NIR) measurements

Absorption spectra were recorded on either a Varian Cary 5 spectrometer or a HP 8453 diode-array spectrometer in Teflon-capped quartz cuvettes (0.1–1.0 cm path length) equipped with side arms. Formation of [**TTF**,**CA**] complex was studied under an argon atmosphere *via* low-temperature (−50 to −95 °C) measurements of the charge-transfer band at $\lambda_{CT} = 1100$ nm (using a Dewar equipped with quartz windows). The intensity of this band ($A_{CT}$) measured in a series of solutions with constant sum of donor and acceptor concentrations (Job's method) showed a clear maximum at the equimolar ratio (inset, Fig. 1). The formation of the 1 : 1 complex was indicated in eqn (4) with equilibrium constant: $K_{CT} = [\mathbf{C}]/\{([\mathbf{D}]° - [\mathbf{C}])([\mathbf{A}]° - [\mathbf{C}])\}$, where [**C**] is the equilibrium concentration of complex, [**D**]° and [**A**]° are the concentrations of donor and acceptor added to the solution. The application of graphical methods by Drago[7] (involving the dependence of $K_{CT}^{-1}$ against $\varepsilon_{CT}$ at different concentrations of donor and acceptor) to the 1100 nm band measured at −68 °C led to the formation constant and extinction coefficient of the precursor complex. Subsequent measurements of $K_{CT}$ at different temperatures resulted in the enthalpy and entropy changes: $\Delta H_{CT}$ and $\Delta S_{CT}$ for the formation of the charge-transfer complex.

## Charge-transfer and photo-excitation of the [TTF,CA] complex

To 2 ml of a 4 mM solution of **TTF** in dichloromethane was added (at −78 °C, under argon) 2 ml of 4 mM solution of **CA** in dichloromethane. Upon mixing, an immediate dark-brown coloration of solution was apparent and the appearance of a strong charge-transfer absorption in the spectral range from 700–1400 nm was measured. The 1.0 cm quartz cuvette was placed in a Dewar (cooled with an acetone–dry ice bath at −78 °C) and irradiated (under argon) with a focused beam through an Corning CS 2–64 filter with a 650 nm cutoff (to excite only charge-transfer transition) from a mercury short arc lamp HBO 500 W/2. [As the thermal control, the same solution was placed in glass tube wrapped with aluminum foil and the tube was kept in the same Dewar.] After 24 h of irradiation, the solution bleached completely but the coloration of the control solution remained unchanged. After removal of the solvent, the crude residue was dissolved in acetonitrile. The HPLC analysis of this solution was performed on an LDC Analytical SM 3100 instrument equipped with a Hypersil BDS C18 reverse-phase column with acetonitrile as eluent. The results of product analysis were the same as those obtained with the thermal reaction carried out room temperature in acetonitrile solution with equimolar quantities of **TTF** and **CA**, in dark, under

argon. In both cases, the [2 + 4] cycloadduct (Chart 1) was obtained in >90% yield.

## X-Ray crystallography

The intensity data for X-ray study were collected at either at −100 °C or −150 °C with a Bruker SMART Apex diffractometer equipped with a CCD detector using Mo-Kα radiation ($\lambda = 0.71073$ Å). The structures were solved by direct methods and refined by full matrix least-squares procedure as described earlier.[33]

Black single crystals of the charge-transfer [1 : 1] complex [**TTF**,**CA**] were prepared by the diffusion of a hexane solution of tetrathiafulvalene into a dichloromethane solution of *o*-chloranil at −65 °C. On the other hand, colorless crystals of the dichloromethane solvate of the [2 + 4] cycloadduct were isolated when the dichloromethane solution containing equimolar quantities of **TTF** and **CA** was covered with hexane and allowed to stand for prolonged periods at −30 °C. Red crystals of the [1 : 1] complex [durene,**CA**] and brown-green crystals of the [3 : 2] complex [pyrene,**CA**] were obtained by evaporation of equimolar dichloromethane solutions of *o*-chloranil with durene and pyrene, respectively. Dark red crystals of the pure **CA** acceptor were prepared either by sublimation or diffusion of hexane into the solution of *o*-chloranil in dichloromethane at −65 °C (β-form). The black crystals of the tetrathiafulvalene cation-radical salt, **TTF⁺•CB⁻**, were prepared by diffusion of hexane into the dichloromethane solution at −65 °C. The dissolution of the **TTF⁺•CB⁻** in diethyl ether at room temperature followed by slow cooling to −30 °C produced single crystals of the ethereal solvate. Structural data are listed in Table 4.

CCDC reference numbers 611965–611972

For crystallographic data in CIF or other electronic format see DOI: 10.1039/b607431f

## Computational methodologies

The reorganization energy for the electron transfer within [**TTF**,**CA**] complex was calculated as a sum of the inner and outer sphere components. The inner-sphere component was calculated as: $\lambda_i = (\lambda_i^{TTF} + \lambda_i^{CA})/2$, where $\lambda_i^{TTF}$ and $\lambda_i^{CA}$ are inner-sphere reorganization energies for the **TTF⁺•**/**TTF** and **CA⁻•**/**CA** redox pairs computed with Gaussian 98 (density-functional theory level, 6–311G* basis, B3LYP functional)[20] as described earlier.[28] The outer-sphere component for the charge-transfer complex [**TTF**,**CA**] was calculated as described earlier in detail for the [**TCNE⁻•**,**TCNE**] complex.[28] For this calculation, [**TTF**,**CA**] was considered as a cavity with an internal dielectric constant of $\varepsilon_{in} = 2$ immersed in a solvent with static and optical dielectric constants $\varepsilon_s$ and $\varepsilon_o$, respectively. The atomic coordinates $r_i$ for the complex were extracted from the X-ray structure of [**TTF**,**CA**]. The charge variations $\Delta e_i$ were determined as the differences of charges on each atom in **TTF**/**TTF⁺•** and **CA**/**CA⁻•** pairs, and the charges on the neutral molecules and the corresponding ion-radicals were calculated with Gaussian 98 (CHELPG option).[20]

To derive eqn (11) (section 3.3), we have taken the following into account: (i) Complex formation involved the interaction of the donor HOMO (occupied by two electrons) and the acceptor LUMO (Chart 2). (ii) Donor–acceptor interaction led to the redistribution of the electron pair (which originally resided on

**Table 4** Crystallographic parameters and the details of the structure refinements

| Compound | [**TTF**,**CA**] | [Durene,**CA**] | [Pyrene,**CA**] | [2 + 4] adduct | **CA** | **CA** (β-form) | **TTF**⁺·CB⁻ | **TTF**⁺·CB·2Et₂O |
|---|---|---|---|---|---|---|---|---|
| Color | Black | Red | Brown-green | Colorless | Red | Red | Brown | Brown |
| Formula | $C_{12}H_4Cl_4O_2S_4$ | $C_{16}H_{14}Cl_4O_2$ | $C_{60}H_{30}Cl_8O_4$ | $C_{26}H_{12}Cl_{12}O_4S_8$ | $C_6Cl_4O_2$ | $C_6Cl_4O_2$ | $C_{19}H_{40}B_{11}S_4$ | $C_{35}H_{80}B_{11}O_4S_4$ |
| $M$ | 450.19 | 380.07 | 1098.44 | 1070.24 | 245.86 | 245.86 | 515.66 | 812.14 |
| Space group | $P2_1/n$ | $P2_1/n$ | $Pc$ | $P2_1/c$ | $P2_1/c$ | $P2_1/n$ | $P2_1/n$ | $P\bar{1}$ |
| $a$/Å | 7.170(3) | 9.1022(5) | 8.3157(4) | 17.000(5) | 6.0592(4) | 26.010(2) | 9.1393(8) | 10.587(5) |
| $b$/Å | 16.961(6) | 13.8161(8) | 38.9670(18) | 13.405(4) | 16.3472(11) | 8.1572(6) | 13.3909(13) | 11.677(5) |
| $c$/Å | 12.731(5) | 13.3595(8) | 14.2436(6) | 17.205(5) | 8.1183(6) | 28.795(2) | 12.5744(10) | 12.740(6) |
| $a$/° | 90 | 90 | 90 | 90 | 90 | 90 | 90 | 63.152(7) |
| $β$/° | 97.176(7) | 100.202(1) | 91.718(1) | 97.907(10) | 94.249(1) | 113.518(4) | 109.609(5) | 67.095(8) |
| $γ$/° | 90 | 90 | 90 | 90 | 90 | 90 | 90 | 68.555(8) |
| $V$/Å³ | 1536.1(10) | 1653.49(16) | 4613.4(4) | 3883(2) | 801.92(10) | 5601.7(8) | 1449.6(2) | 1259.4(10) |
| $Z$ | 4 | 4 | 4 | 4 | 4 | 28 | 2 | 1 |
| $F(000)$ | 896 | 776 | 2232 | 2128 | 480 | 3360 | 546 | 441 |
| $ρ$/g cm⁻³ | 1.947 | 1.527 | 1.581 | 1.831 | 2.036 | 2.041 | 1.181 | 1.071 |
| Refls | 5633 | 5361 | 26525 | 8301 | 8492 | 48388 | 13301 | 19065 |
| Indpndt | 3901 | 5361 | 26525 | 6663 | 2570 | 16756 | 4128 | 7248 |
| Obsd ($F > 4σ$) | 2142 | 4919 | 24099 | 3800 | 2293 | 7532 | 3505 | 5370 |
| $R_1$ ($F > 4σ$) | 0.0485 | 0.0362 | 0.0478 | 0.0564 | 0.0393 | 0.0596 | 0.0454 | 0.0485 |
| w$R_2$ | 0.0900 | 0.0947 | 0.1074 | 0.1075 | 0.1017 | 0.1561 | 0.1292 | 0.1363 |
| GOF | 0.773 | 1.044 | 1.058 | 0.835 | 1.056 | 0.989 | 1.109 | 0.985 |

the donor HOMO), such that the ground-state wave function $\Psi_{GS}$ contained the contribution of the acceptor LUMO (represented by the coefficient $b$). (iii) The coefficients in eqn (6) were normalized as: $a^2 + b^2 = 1$. Accordingly, the fraction of charge transferred from the donor to the acceptor represented the integral electron density of the molecular ground-state wave-function $\Psi_{GS}$ residing on the acceptor site, and it was expressed as: $q = 2b^2$. Therefore, the coefficients in eqn (6) were presented as: $b = (q/2)^{1/2}$ and $a = (1 - q/2)^{1/2}$. Together with the substitution of the excited- and ground-state energy difference by $v_{CT}$, eqn (9) was rewritten as: $(q/2)^{1/2}(1 - q/2)^{1/2} = H_{ab}/v_{CT}$. The latter relationship led to the expression of the electronic coupling element in eqn (11) *via* the value of $q$ (experimentally measured X-ray structures of the donor and acceptor moieties within the [**TTF**,**CA**] complex) and the energy of the NIR-band ($v_{CT}$).

## Acknowledgements

## References

1 R. S. Mulliken and W. B. Person, *Molecular Complexes*, Wiley, N.Y., 1969.
2 R. Foster, *Organic Charge-Transfer Complexes*, Academic, N.Y., 1969; G. Briegleb, *Electronen-Donator-Acceptor Komplexes*, Springer, Berlin, 1961.
3 N. Sutin, Theory of Electron Transfer Reactions: Insights and Hindsights, *Prog. Inorg. Chem.*, 1983, **30**, 441–498.
4 (*a*) R. S. Davidson, Photochemical Reactions Involving Charge-Transfer Complexes, in *Molecular Association*, ed. R. Foster, Academic, New York, 1975, vol. 1, ch. 4, pp. 215–334; (*b*) See also: J. K. Kochi, Electron transfer in the thermal and photochemical activation of electron donor–acceptor complexes in organic and organometallic reactions, *Adv. Phys. Org. Chem.*, 1994, **29**, 185–272; E. Bosch, S. M. Hubig and J. K. Kochi, Paterno–Büchi Coupling of (Diaryl)acetylenes

and Quinone *via* Photoinduced Electron Transfer, *J. Am. Chem. Soc.*, 1998, **120**, 386–395.
5 *TTF Chemistry: Fundamentals and Applications of Tetrathiafulvalene*, ed. J.-I. Yamada and T. Sugimoto, Kodansha Springer, Berlin, 2004.
6 C. K.-F. Shen, H. M. Duong, G. Sonmez and F. Wudl, Novel Reversible Ionic-to-Covalent Transition in a Highly Conducting TTF Derivative, *J. Am. Chem. Soc.*, 2003, **125**, 16206–16207.
7 R. S. Drago, *Physical Methods in Chemistry*, Saunders Co, Philadelphia, 1977.
8 B. Chakraborty, A. K. Mukherjee and B. K. Seal, Charge-transfer complex formation between *o*-chloranil and a series of polynuclear aromatic hydrocarbons, *Spectrochim. Acta, Part A*, 2001, **57A**, 223–229; B. Chakravarty, K. Datta, A. K. Mukherjee, M. Banerjee and B. K. Seal, Studies on the charge-transfer complexes of *o*-chloranil with a series of methylbenzenes, *Indian J. Chem. A*, 1998, **37A**, 865–870.
9 V. Ganesan, S. V. Rosokha and J. K. Kochi, Isolation of the Latent Precursor Complex in Electron-Transfer Dynamics. Intermolecular Association and Self-Exchange with Acceptor Anion Radicals, *J. Am. Chem. Soc.*, 2003, **125**, 2559–2571.
10 D. Sun, S. V. Rosokha and J. K. Kochi, Donor–Acceptor (Electronic) Coupling in the Precursor Complex to Organic Electron Transfer: Intermolecular and Intramolecular Self-Exchange between Phenothiazine Redox Centers, *J. Am. Chem. Soc.*, 2004, **126**, 1388–1401; D. Sun, S. V. Rosokha, S. V. Lindeman and J. K. Kochi, Intervalence (Charge-Resonance) Transitions in Organic Mixed-Valence Systems. Through-Space *versus* Through-Bond Electron Transfer between Bridged Aromatic (Redox) Centers, *J. Am. Chem. Soc.*, 2003, **125**, 15950–15963; See also: S. V. Rosokha and J. K. Kochi, Molecular and Electronic Structure of the Long-Bonded π-Dimers of Tetrathiafulvalene Cation Radical in Intermolecular Electron Transfer and (Solid-State) Conductivity, *J. Am. Chem. Soc.*, submitted for publication.
11 *Cambridge Structural Database, Version 5.27*, Cambridge Crystallographic Data Centre, 2005.
12 C. K. Prout and B. Kamenar, Crystal structures of electron-donor–acceptor complexes, in *Molecular Complexes*, ed. R. Foster, Crane, Russak & Co, New York, 1973, vol. 1, ch. 4, pp. 151–208; Z. G. Soos and D. J. Klein, Charge transfer in solid state complexes, in *Molecular Association*, ed. R. Foster, Academic, New York, 1975 vol. 1, ch. 1, pp. 1–109.
13 M. R. Bryce, S. R. Davies, M. B. Hursthouse and M. Motevalli, Preparation, solid-state characterization and X-ray crystal structure of a 1 : 1 complex of tetrathiafulvalene and *m*-dinitrobenzene (TTF–*m*DNB), *J. Chem. Soc., Perkin Trans. 2*, 1988, 1713–1716.
14 G. M. Frankenbach, M. A. Beno and J. M. Williams, Charge-transfer complex of 2,2′,5,5′-tetrathiafulvalene and *p*-benzoquinone, *Acta Crystallogr., Sect. C: Cryst. Struct. Commun.*, 1991, **C47**, 762–764.

15 M. Le Cointe, M. H. Lemee-Cailleau, H. Cailleau, B. Toudic, L. Toupet, G. Heger, F. Moussa, P. Schweiss, K. H. Kraft and N. Karl, Symmetry breaking and structural changes at the neutral-to-ionic transition in tetrathiafulvalene-*p*-chloranil, *Phys. Rev. B: Condens. Matter*, 1995, **51**, 3374–3386.

16 B. T. King, B. C. Noll, A. J. McKinley and J. Michl, Dodecamethylcarba-*closo*-dodecaboranyl (CB11Me12.bul.), a Stable Free Radical, *J. Am. Chem. Soc.*, 1996, **118**, 10902–10903.

17 D. A. Clemente and A. Marzotto, Structure of two polymorphs of the TTF–TCNE charge-transfer complex and the degree of ionicity, *J. Mater. Chem.*, 1996, **6**, 941–946.

18 W. F. Cooper, J. W. Edmonds, F. Wudl and P. Coppens, The 2-2′-bi-1,3-dithiole, *Cryst. Struct. Commun.*, 1974, **3**, 23–26.

19 T. C. Umland, S. Allie, T. Kuhlmann and P. Coppens, Relation between Geometry and Charge Transfer in Low-Dimensional Organic Salts, *J. Phys. Chem.*, 1988, **92**, 6456–6460.

20 M. J. Frisch, G. W. Trucks, H. B. Schlegel, G. E. Scuseria, M. A. Robb, J. R. Cheeseman, V. G. Zakrzewski, J. A. Montgomery, Jr., R. E. Stratmann, J. C. Burant, S. Dapprich, J. M. Millam, A. D. Daniels, K. N. Kudin, M. C. Strain, O. Farkas, J. Tomasi, V. Barone, M. Cossi, R. Cammi, B. Mennucci, C. Pomelli, C. Adamo, S. Clifford, J. Ochterski, G. A. Petersson, P. Y. Ayala, Q. Cui, K. Morokuma, P. Salvador, J. J. Dannenberg, D. K. Malick, A. D. Rabuck, K. Raghavachari, J. B. Foresman, J. Cioslowski, J. V. Ortiz, A. G. Baboul, B. B. Stefanov, G. Liu, A. Liashenko, P. Piskorz, I. Komaromi, R. Gomperts, R. L. Martin, D. J. Fox, T. Keith, M. A. Al-Laham, C. Y. Peng, A. Nanayakkara, M. Challacombe, P. M. W. Gill, B. G. Johnson, W. Chen, M. W. Wong, J. L. Andres, C. Gonzalez, M. Head-Gordon, E. S. Replogle and J. A. Pople, *GAUSSIAN 98 (Revision A.11)*, Gaussian, Inc., Pittsburgh, PA, 2001.

21 L. Pauling, *Nature of the Chemical Bond*, Cornell, Ithaca, NY, 1960.

22 S. V. Lindeman, S. V. Rosokha, D. Sun and J. K. Kochi, X-Ray Structure Analysis and the Intervalent Electron Transfer in Organic Mixed-Valence Crystals with Bridged Aromatic Cation Radicals, *J. Am. Chem. Soc.*, 2002, **124**, 843–855; J. M. Lu, S. V. Rosokha, S. V. Lindeman, I. S. Neretin and J. K. Kochi, Separated" *versus* "Contact" Ion-Pair Structures in Solution from Their Crystalline States: Dynamic Effects on Dinitrobenzenide as a Mixed-Valence Anion, *J. Am. Chem. Soc.*, 2005, **127**, 1797–1809.

23 C. Creutz, M. D. Newton and N. Sutin, Metal–ndash and metal–metal coupling element, *J. Photochem. Photobiol., A*, 1994, **82**, 47–59.

24 M. D. Newton, Electron transfer: theoretical models and computational implementation, in *Electron Transfer in Chemistry*, ed. V. Balzani, Wiley-VCH, New York, 2001, vol. 1, pp. 3–63.

25 N. S. Hush, Intervalence-transfer absorption. II. Theoretical considerations and spectroscopic data, *Prog. Inorg. Chem.*, 1967, **8**, 391–444; N. S. Hush, Homogeneous and heterogeneous optical and thermal electron transfer, *Electrochim. Acta*, 1968, **13**, 1005–1023.

26 B. S. Brunschwig and N. Sutin, Energy surfaces, reorganization energies and coupling elements in electron transfer, *Coord. Chem. Rev.*, 1999, **187**, 233–254; B. S. Brunschwig and N. Sutin, N. Reflections on the two-state electron-transfer model, in *Electron Transfer in Chemistry*, ed. V. Balzani, Wiley, New York, 2001, vol. 2, pp. 583–617.

27 R. A. Marcus and N. Sutin, Electron Transfer in Chemistry and Biology, *Biochim. Biophys. Acta*, 1985, **811**, 265–322; R. A. Marcus, On the theory of oxidation-reduction reactions involving electron transfer. Comparison and properties of electrochemical and chemical rate constants, *J. Phys. Chem.*, 1963, **67**, 853–857.

28 S. V. Rosokha, J.-M. Lü, M. D. Newton and J. K. Kochi, Intermolecular Electron-Transfer Mechanisms *via* Quantitative Structures and Ion-Pair Equilibria for Self-Exchange of Anionic (Dinitrobenzenide) Donors, *J. Am. Chem. Soc.*, 2005, **127**, 7411–7420; S. V. Rosokha, M. D. Newton, M. Head-Gordon and J. K. Kochi, Mulliken–Hush elucidation of the encounter (precursor) complex in intermolecular electron transfer *via* self-exchange of tetracyanoethylene anion-radical, *Chem. Phys.*, 2006, **324**, 117–128.

29 M. V. Vener, N. T. Ioffe, A. V. Cheprakov and V. G. Mairanovsky, Theoretical study of homogeneous electron self-exchange in polar aromatic molecules: the role of the reactant structure, *J. Electroanal. Chem. Interfacial Electrochem.*, 1994, **370**, 33–39.

30 M. Robin and P. Day, Mixed valence chemistry. A survey and classification, *Adv. Inorg. Chem. Radiochem.*, 1967, **10**, 247–422.

31 S. V. Rosokha and J. K. Kochi, Mechanism of Inner-Sphere Electron Transfer *via* Charge-Transfer (Precursor) Complexes. Redox Energetics of Aromatic Donors with the Nitrosonium Acceptor, *J. Am. Chem. Soc.*, 2001, **123**, 8985–8999; S. V. Rosokha and J. K. Kochi, Strong electronic coupling in intermolecular (charge-transfer) complexes. Mechanistic relevance to thermal and optical electron transfer from aromatic donors, *New J. Chem.*, 2002, **26**, 851–860.

32 H. Taube, H. Myers and R. L. Rich, The mechanism of electron transfer in solution, *J. Am. Chem. Soc.*, 1953, **75**, 4118–4119; H. Taube, Mechanisms of oxidation–reduction reactions, *J. Chem. Educ.*, 1968, **45**, 452–461.

33 S. Steenken, One-electron redox reactions between radicals and organic molecules. An addition/elimination (inner-sphere) path, *Top. Curr. Chem.*, 1996, **177**, 125–145.

34 D. Small, V. Zaitsev, Y. Jung, S. V. Rosokha, M. Head-Gordon and J. K. Kochi, Intermolecular π-to-π Bonding between Stacked Aromatic Dyads. Experimental and Theoretical Binding Energies and Near-IR Optical Transitions for Phenalenyl Radical/Radical *versus* Radical/Cation Dimerizations, *J. Am. Chem. Soc.*, 2004, **126**, 13850–13858; J.-M. Lu, S. V. Rosokha and J. K. Kochi, Stable (Long-Bonded) Dimers *via* the Quantitative Self-Association of Different Cationic, Anionic, and Uncharged π-Radicals: Structures, Energetics, and Optical Transitions. Mechanism of Inner-Sphere Electron Transfer *via* Charge-Transfer (Precursor) Complexes. Redox Energetics of Aromatic Donors with the Nitrosonium Acceptor, *J. Am. Chem. Soc.*, 2003, **125**, 12161–12171.

35 A. Pross, The single electron shift as a fundamental process in organic chemistry: the relationship between polar and electron-transfer pathways, *Acc. Chem. Res.*, 1985, **18**, 212–219.

36 S. M. Hubig and J. K. Kochi, Direct Observation of the Wheland Intermediate in Electrophilic Aromatic Substitution. Reversible Formation of Nitrosoarenium Cations, *J. Am. Chem. Soc.*, 2000, **122**, 8279–8288.